

## Quark level linear $\sigma$ model ( $L\sigma M$ ) via loop graphs

M.D. SCADRON

*Physics Department, University of Arizona, Tucson, AZ, 85721 USA*

First, the  $L\sigma M$  is nonperturbatively solved via loop-order gap equations. Then the Nambu-Goldstone theorem (NGT) is expressed in  $L\sigma M$  language. Next, the Lee null tadpole sum for this  $SU(2)$   $L\sigma M$  theory is shown to require  $N_c = 3$ . Then  $L\sigma M$  s-wave chiral cancellations are studied in tree-and in loop-order. Also, vector meson dominance (VMD) is shown to follow from this  $L\sigma M$ . Next, the scalar nonet is studied in the infinite momentum frame (IMF). Finally, the  $L\sigma M$  is suggested as the infrared limit of nonperturbative QCD.

*Invited Talk at the scalar meson workshop, Kyoto, June 2000*

### §1. Introduction

To begin, we give the original<sup>1)</sup> tree-level chiral-broken  $SU(2)$  interacting  $L\sigma M$  lagrangian density, but after the spontaneous symmetry breaking (SSB) shift:

$$\mathcal{L}_{L\sigma M}^{int} = g\bar{\Psi}(\sigma' + i\gamma_5 \boldsymbol{\tau} \cdot \boldsymbol{\pi})\Psi + g'\sigma'(\sigma'^2 + \boldsymbol{\pi}^2) - \lambda(\sigma'^2 + \boldsymbol{\pi}^2)^2/4. \quad (1\cdot1)$$

In refs.1) the couplings  $g$ ,  $g'$ ,  $\lambda$  in (1·1) satisfy the quark-level Goldberger-Treiman relation (GTR) for  $f_\pi \approx 93$  MeV and  $f_\pi \sim 90$  MeV in the chiral limit (CL):

$$g = m_q/f_\pi, \quad g' = m_\sigma^2/2f_\pi = \lambda f_\pi. \quad (1\cdot2)$$

We work in loop order and dynamically generate mass terms in (1·1) via non-perturbative Nambu-type gap equations  $\delta f_\pi = f_\pi$ ,  $\delta m_q = m_q$ . The CL  $m_\pi = 0$ , corresponds to  $\langle 0|\partial A|\pi \rangle = 0$  for  $\langle 0|A_\mu^3|\pi^0 \rangle = if_\pi q_\mu$ . The latter requires the GTR  $m_q = f_\pi g$  to be valid in tree and loop order, fixing  $g$ ,  $g'$ ,  $\lambda$  in loop order.

In §2, 3, this quark-level  $L\sigma M$  is nonperturbatively solved via loop-order gap equations. In §4, the NGT is expressed in  $L\sigma M$  language with charge radius  $r_\pi = 1/m_q$  characterizing quark fusion for the tightly bound  $q\bar{q}$  pion. In §5, the Lee null tadpole sum is shown to require  $N_c = 3$  for the true vacuum. §6 discusses *s*-wave chiral cancellations in the  $L\sigma M$ . §7 shows VMD follows directly from the  $L\sigma M$ . §8 studies the scalar meson nonet in the IMF. Finally §9 suggests this  $L\sigma M$  is the infrared limit of nonperturbative QCD. We give our conclusions in §10.

### §2. Quark loop gap equations

First we compute  $\delta f_\pi = f_\pi$  in the CL via the *u* and *d* quark loops of Fig.1a. Replacing  $f_\pi$  by  $m_q/g$  and taking the quark trace, giving  $4m_q q_\mu$ , the factors  $m_q q_\mu$  cancel, requiring the CL log-divergent gap equation (LDGE)<sup>2), 3)</sup>,  $\bar{d}^4 p = d^4 p/(2\pi)^4$ :

$$1 = -4iN_c g^2 \int (p^2 - m_q^2)^{-2} \bar{d}^4 p. \quad (2\cdot1)$$

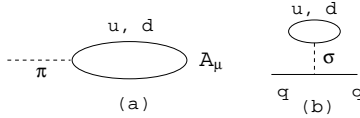


Fig. 1. Quark loop for  $f_\pi$ (a), quark tadpole loop for  $m_q$ (b)

Anticipating  $g \sim 320$  MeV/90MeV  $\sim 3.6$  from the CL GTR, this LDGE (2.1) suggests an UV cutoff  $\Lambda \sim 750$  MeV. Such a 750 MeV cutoff separates L $\sigma$ M elementary particle  $\sigma(600) < \Lambda$  from bound states  $\rho(770)$ ,  $\omega(780)$ ,  $a_1(1260) > \Lambda$ . This is a  $Z = 0$  compositeness condition<sup>4)</sup>, requiring  $g = 2\pi/\sqrt{N_c}$ . We later derive this from our dynamical symmetry breaking (DSB) loop order L $\sigma$ M.

Next we study  $\delta m_q = m_q$  in the CL, with zero current quark mass;  $m_q$  is the nonstrange constituent quark mass. The needed mass gap is formed via the quadratically divergent quark tadpole loop of Fig.1b; additional quark  $\pi$ - and  $\sigma$ -mediated self-energy graphs then cancel<sup>3)</sup>, giving the quadratic divergent mass gap

$$1 = 8iN_c g^2 / (-m_\sigma^2) \cdot \int (p^2 - m_q^2)^{-1} \bar{d}^4 p. \quad (2.2)$$

Here the  $q^2 = 0$  tadpole  $\sigma$  propagator  $(0 - m_\sigma^2)^{-1}$  means the right-hand side (rhs) of the integral in eq.(2.2) acts as a counterterm quadratic divergent NJL<sup>5)</sup> mass gap.

References 3) first subtract the quadratic-from the log-divergent integrals of eqs. (2.1), (2.2) to form the dimensional regularization (dim. reg.) lemma for  $2l = 4$ :

$$\int \bar{d}^4 p \left[ \frac{m_q^2}{(p^2 - m_q^2)^2} - \frac{1}{p^2 - m_q^2} \right] = \lim_{l \rightarrow 2} \frac{im_q^{2l-2}}{(4\pi)^l} [\Gamma(2-l) + \Gamma(1-l)] = \frac{-im_q^2}{(4\pi)^2}. \quad (2.3)$$

This dim. reg. lemma (2.3) follows because  $\Gamma(2-l) + \Gamma(1-l) \rightarrow -1$  as  $l \rightarrow 2$  due to the gamma function defining identity  $\Gamma(z+1) = z\Gamma(z)$ . This lemma eq.(2.3) is more general than dim. reg.; (i) use partial fractions to write

$$\frac{m^2}{(p^2 - m^2)^2} - \frac{1}{p^2 - m^2} = \frac{1}{p^2} \left[ \frac{m^4}{(p^2 - m^2)^2} - 1 \right], \quad (2.4)$$

- (ii) integrate eq.(2.4) via  $\bar{d}^4 p$  and neglect the latter massless tadpole  $\int \bar{d}^4 p/p^2 = 0$  (as is also done in dim. reg., analytic, zeta function and Pauli-Villars regularization<sup>3)</sup>)
- (iii) Wick rotate  $d^4 p = i\pi^2 p_E^2 dp_E^2$  in the integral over eq.(2.4) to find

$$\int \bar{d}^4 p \left[ \frac{m^2}{(p^2 - m^2)^2} - \frac{1}{p^2 - m^2} \right] = -\frac{im^4}{(4\pi)^2} \int_0^\infty \frac{dp_E^2}{(p_E^2 + m^2)^2} = \frac{-im^2}{(4\pi)^2}. \quad (2.5)$$

So (2.5) gives the dim.reg.lemma (2.3); both are *regularization scheme independent*.

Following refs.3) we combine eqs. (2.3) or (2.5) with the LDGE (2.1) to solve the quadratically divergent mass gap integral (2.2) as

$$m_\sigma^2 = 2m_q^2(1 + g^2 N_c / 4\pi^2). \quad (2.6)$$

Also the Fig.2 quark bubble plus tadpole graphs dynamically generate the  $\sigma$  mass<sup>3)</sup>:



Fig. 2. Quark bubble plus quark tadpole loop for  $m_\sigma^2$ .

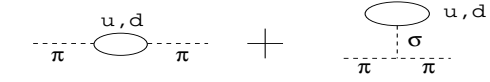


Fig. 3. Quark bubble plus quark tadpole loop for  $m_\pi^2$ .



Fig. 4. Quark triangle shrinks to point for  $m_\sigma \rightarrow \pi\pi$ .

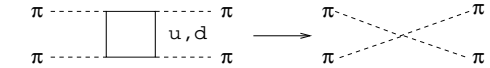


Fig. 5. Quark box shrinks to point contact for  $\pi\pi \rightarrow \pi\pi$ .

$$m_\sigma^2 = 16iN_c g^2 \int \bar{d}^4 p \left[ \frac{m_q^2}{(p^2 - m_q^2)^2} - \frac{1}{p^2 - m_q^2} \right] = \frac{N_c g^2 m_q^2}{\pi^2}, \quad (2.7)$$

where we have deduced the rhs of eq.(2.7) by using (2.3) or (2.5). Finally solving the two equations (2.6) and (2.7) for the two unknowns  $m_\sigma^2/m_q^2$  and  $g^2 N_c$ , one finds<sup>3)</sup>

$$m_\sigma = 2m_q, \quad g = 2\pi/\sqrt{N_c}. \quad (2.8)$$

Not surprisingly, the lhs equation in (2.8) is the famous NJL four quark result<sup>5)</sup>, earlier anticipated for the L $\sigma$ M in refs.6). The rhs equation in (2.8) is also the consequence of the Z=0 compositeness condition<sup>4)</sup>, as noted earlier.

Finally we compute  $m_\pi^2$  from the analog pion bubble plus tadpole graphs of Fig.3. Since both quark loops (ql) are quadratic divergent in the CL, one finds<sup>2),3)</sup>

$$m_{\pi,ql}^2 = 4iN_c [2g^2 - 4gg'm_q/m_\sigma^2] \int (p^2 - m_q^2)^{-1} \bar{d}^4 p = 0; \quad g' = m_\sigma^2/2f_\pi, \quad (2.9)$$

using the GTR. Not surprisingly, eq.(2.9) is the dynamical version of the SSB (1.2).

### §3. Loop order three- and four-point functions

Having studied all 2-point functions in §2, we now look at 3- and 4-point functions. In the CL the  $u$  and  $d$  quark loops of Fig.4 generate  $g_{\sigma\pi\pi}$ <sup>2),3)</sup> as

$$g_{\sigma\pi\pi} = -8ig^3 N_c m_q \int (p^2 - m_q^2)^{-2} \bar{d}^4 p = 2gm_q \quad (3.1)$$

by virtue of the LDGE (2.1). Using the GTR and  $m_\sigma = 2m_q$ , eq.(3.1) reduces to

$$g_{\sigma\pi\pi} = 2gm_q = m_\sigma^2/2f_\pi = g'. \quad (3.2)$$

In effect, the  $g_{\sigma\pi\pi}$  loop of Fig.4 “shrinks” to the L $\sigma$ M cubic meson coupling  $g'$  in the tree-level lagrangian eq.(1.1), but only when  $m_\sigma = 2m_q$  and  $g/m_q = 1/f_\pi$ .

Next we study the 4-point  $\pi\pi$  quark box of Fig.5, giving a CL log divergence<sup>3)</sup>:

$$\lambda_{box} = -8iN_c g^4 \int (p^2 - m_q^2)^{-2} \bar{d}^4 p = 2g^2 = g'/f_\pi = \lambda_{tree}, \quad (3.3)$$

employing the LDGE (2.1) to reduce (3.3) to  $2g^2$ . Equation(3.3) shrinks to  $\lambda_{tree}$ , by virtue of eq.(1.2). Substituting (2.8) into (3.3), we find  $\lambda = 8\pi^2/N_c$ .

We have dynamically generated the entire L $\sigma$ M lagrangian (1.1), but using the DSB true vacuum, satisfying specific values of  $g$ ,  $g'$ ,  $\lambda$  in eq.(1.1).

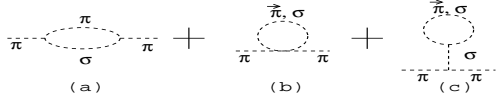


Fig. 6. Meson bubble(a) meson quartic (b) meson tadpole(c) graphs for  $m_\pi^2$ .

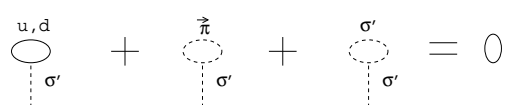


Fig. 7. Null tadpole sum for SU(2)  $L\sigma M$ .

#### §4. Nambu-Goldstone theorem (NGT) in $L\sigma M$ loop order

Having dynamically generated the chiral pion and  $\sigma$  as elementary, we must add to Fig.3 the five meson loops of Fig.6. The first bubble graph in Fig.6 is log divergent, while the latter four quartic and tadpole graphs are quadratic divergent.

To proceed, first one uses a partial fraction identity to rewrite the log-divergent bubble graph as the difference of  $\pi$  and  $\sigma$  quadratic divergent integrals<sup>2), 7)</sup>. Then the six meson loops (ml) of Fig.6 can be separated into three quadratic divergent  $\pi$  and three quadratic divergent  $\sigma$  integrals<sup>7)</sup>:

$$m_{\pi,ml}^2 = (-2\lambda + 5\lambda - 3\lambda)i \int (p^2 - m_\pi^2)^{-1} \bar{d}^4 p + (2\lambda + \lambda - 3\lambda)i \int (p^2 - m_\sigma^2)^{-1} \bar{d}^4 p. \quad (4.1)$$

Adding eq.(4.1) to eq.(2.9), the total  $m_\pi^2$  in the CL is in loop order

$$m_\pi^2 = m_{\pi,ql}^2 + m_{\pi,\pi l}^2 + m_{\pi,\sigma l}^2 = 0 + 0 + 0 = 0. \quad (4.2)$$

Moreover, eq.(4.2) is chirally regularized and renormalized because the tadpole graphs of Figs.3, 6c are already counterterm masses acting as subtraction constants.

A second aspect of the chiral pion concerns the pion charge radius  $r_\pi$  in the CL. First one computes the pion form factor  $F_{\pi,ql}(q^2)$  due to quark loops (ql) and then differentiates it with respect to  $q^2$  at  $q^2 = 0$  to find  $r_{\pi,ql}^2$  as

$$\begin{aligned} r_{\pi,ql}^2 &= \frac{6dF_{\pi,ql}(q^2)}{dq^2} \Big|_{q^2=0} = 8iN_c g^2 \int_0^1 dx 6x(1-x) \int (p^2 - m_q^2)^{-3} \bar{d}^4 p \\ &= 8iN_c (4\pi^2/N_c) \cdot (-i\pi^2/2m_q^2 16\pi^4) = 1/m_q^2. \end{aligned} \quad (4.3)$$

Although  $r_\pi$  was originally expressed as  $\sqrt{N_c}/2\pi f_\pi$ <sup>8), 7)</sup>, we prefer the result (4.3) or  $r_\pi = 1/m_q$ , as it requires the tightly bound  $q\bar{q}$  pion to have the two quarks fused in the CL. Later we will show that  $N_c = 3$ ;  $m_q \approx 325$  MeV in the CL gives  $r_\pi = 1/m_q \approx 0.6$  fm. The observed  $r_\pi$  is<sup>9)</sup>  $(0.63 \pm 0.01)$  fm. The alternative ChPT requires  $r_\pi \propto L_9$ , a low energy constant (LEC)! However VMD successfully predicts

$$r_\pi^{VMD} = \sqrt{6}/m_\rho \approx 0.63 \text{ fm}, \quad (4.4)$$

not only accurate but  $r_\pi^{VMD}$  and  $r_\pi^{L\sigma M}$  in (4.3) and (4.4) are clearly related<sup>7)</sup>.

#### §5. Lee null tadpole sum in SU(2) $L\sigma M$ finding $N_c = 3$

To characterize the true DSB (not the false SSB) vacuum, B. Lee<sup>10)</sup> requires the sum of loop-order tadpoles to vanish, see eg. our Fig.7. This tadpole sum is<sup>3)</sup>

$$<\sigma'> = 0 = -i8N_c g m_q \int (p^2 - m_q^2)^{-1} \bar{d}^4 p + 3ig' \int (p^2 - m_\sigma^2)^{-1} \bar{d}^4 p. \quad (5.1)$$

Replacing  $g$  by  $m_q/f_\pi$ ,  $g'$  by  $m_\sigma^2/2f_\pi$  and scaling the quadratic divergent  $q$ (or  $\sigma$ ) loop integrals by  $m_q^2$  (or  $m_\sigma^2$ ), eq.(5·1) requires<sup>3)</sup> (neglecting the pion tadpole)

$$N_c(2m_q)^4 = 3m_\sigma^4. \quad (5\cdot2)$$

But we know from eq.(2·8) that  $2m_q = m_\sigma$ , so the loop-order SU(2) LσM result (5·2) in turn *predicts*  $N_c = 3$ , a satisfying result ! Then the dynamically generated SU(2) loop-order LσM in §3 also predicts in the CL<sup>3)</sup>  $m_q \approx 325$  MeV,  $m_\sigma \approx 650$  MeV and  $g = 2\pi/\sqrt{3} = 3.6276$ ,  $g' = 2gm_q \approx 2.36$  GeV,  $\lambda = 8\pi^2/3 \approx 26.3$ .

## §6. Chiral $s$ -wave cancellations in LσM

Away from the CL, the tree-order LσM requires the cubic meson coupling to be

$$g_{\sigma\pi\pi} = (m_\sigma^2 - m_\pi^2)/2f_\pi = \lambda f_\pi. \quad (6\cdot1)$$

But at threshold  $s = m_\pi^2$ , so the net  $\pi\pi$  amplitude then vanishes using (6·1):

$$M_{\pi\pi} = M_{\pi\pi}^{contact} + M_{\pi\pi}^{\sigma pole} \rightarrow \lambda + 2g_{\sigma\pi\pi}^2(m_\pi^2 - m_\sigma^2)^{-1} = 0. \quad (6\cdot2)$$

In effect, the contact  $\lambda$  “chirally eats” the  $\sigma$  pole at the  $\pi\pi$  threshold at tree level. Then  $\sigma$  poles from the cross channels predict a LσM Weinberg PCAC form<sup>11), 12)</sup>

$$\begin{aligned} M_{\pi\pi}^{abcd} &= A\delta^{ab}\delta^{cd} + B\delta^{ac}\delta^{bd} + C\delta^{ad}\delta^{bc}, \\ A^{L\sigma M} &= -2\lambda \left[ 1 - \frac{2\lambda f_\pi^2}{m_\sigma^2 - s} \right] = \left( \frac{m_\sigma^2 - m_\pi^2}{m_\sigma^2 - s} \right) \left( \frac{s - m_\pi^2}{f_\pi^2} \right). \end{aligned} \quad (6\cdot3)$$

So the I=0  $s$ -channel amplitude  $3A+B+C$  at threshold predicts a 23% enhancement of the Weinberg  $s$ -wave I=0 scattering length at  $s = 4m_\pi^2$ ,  $t = u = 0$  for  $m_\sigma \approx 650$  MeV with  $\epsilon = m_\pi^2/m_\sigma^2 \approx 0.045$  and<sup>12)</sup> (using only eq.(6·3))

$$a_{\pi\pi}^{(0)}|_{L\sigma M} = \left( \frac{7 + \epsilon}{1 - 4\epsilon} \right) \frac{m_\pi}{32\pi f_\pi^2} \approx (1.23) \frac{7m_\pi}{32\pi f_\pi^2} \approx 0.20m_\pi^{-1}. \quad (6\cdot4)$$

For a  $\sigma(550)$  and  $\epsilon \approx 0.063$  this LσM scattering length (6·4) increases to  $0.22m_\pi^{-1}$ . Compare this simple LσM tree order result (6·4) with the analogue ChPT  $0.22m_\pi^{-1}$  scattering length requiring a 2-loop calculation involving about 100 LECs ! These  $\pi\pi$  scattering length problems should be sorted out soon by R. Kamiński, *et. al.*<sup>13)</sup>.

In LσM loop order the analog cancellation is due to a Dirac matrix *identity*<sup>14)</sup>:

$$(\gamma \cdot p - m)^{-1} 2m\gamma_5 (\gamma \cdot p - m)^{-1} = -\gamma_5 (\gamma \cdot p - m)^{-1} - (\gamma \cdot p - m)^{-1} \gamma_5. \quad (6\cdot5)$$

At a soft pion momentum, eq.(6·5) requires a  $\sigma$  meson to be “eaten” via a quark box-quark triangle cancellation for  $a_1 \rightarrow \pi(\pi\pi)$   $s$  wave,  $\gamma\gamma \rightarrow 2\pi^0$ ,  $\pi^- p \rightarrow \pi\pi n$  as suggested in each case by low energy data<sup>14), 15)</sup>. Also a soft pion scalar kappa  $\kappa(800-900)$  is “eaten” in  $K^- p \rightarrow K^- \pi^+ n$  peripheral scattering<sup>15)</sup>.

As for resonant  $\pi\pi$  phase shifts, the needed  $s$ -wave chiral cancellation of eq.(6·2) must have an analog  $s$ -wave  $\pi\pi$  phase shift effect. S. Ishida et. al.<sup>16)</sup> suggest



Fig. 8. Quark triangle graphs contributing to  $\rho^0 \rightarrow \pi\pi$ .

this chiral cancellation corresponds to subtracting a background phase  $-\delta_{BG} = p_\pi^{CM} r_c$ , where  $r_c$  is near the observed pion charge radius of 0.63 fm in eq.(4·3) for the LσM. Then CERN-Munich modified  $\pi\pi$  phase shifts appear to approach 90 deg., corresponding to a resonant  $\sigma(550\text{-}600)$ . This resonant  $\sigma \rightarrow \pi^+\pi^-$  width is<sup>16)</sup>

$$\Gamma_R(s) = p_\pi^{CM}(8\pi s)^{-1}|g_R F(s)|^2 \approx 340\text{MeV at } \sqrt{s_R} \approx 600\text{MeV}, g_R \approx 3.6\text{GeV (6·6)}$$

for  $p_\pi^{CM} = \sqrt{s/4 - m_\pi^2} \approx 260$  MeV. Then the total  $\sigma\pi^+\pi^-$ ,  $\sigma\pi^0\pi^0$  width is  $\Gamma_{\sigma\pi\pi} \approx 3/2 \cdot 340$  MeV = 510 MeV. Also this  $g_R$  is double the LσM coupling (6·1)<sup>12)</sup>:

$$g_R \rightarrow 2g_{\sigma\pi\pi} = (m_\sigma^2 - m_\pi^2)/f_\pi \approx 3.67\text{GeV}, \quad (6·7)$$

close to  $g_R \approx 3.6$  GeV in eq.(6·6). Furthermore the LσM total decay width is<sup>17)</sup>

$$\Gamma_{\sigma\pi\pi}^{L\sigma M} = (3/2) \cdot (p_\pi^{CM}/8\pi) \cdot (|2g_{\sigma\pi\pi}|^2/m_\sigma^2) \approx 580\text{MeV, for } m_\sigma^R \approx 600\text{MeV (6·8)}$$

## §7. VMD and the LσM

Given the implicit LDGE (2·1) UV cutoff  $\Lambda \approx 750$  MeV, the  $\rho(770)$  can be taken as an external field (bound state  $\bar{q}q$  vector meson). Accordingly the quark loop graphs of Fig.8 generate the loop order  $\rho\pi\pi$  coupling<sup>2),3)</sup>

$$g_{\rho\pi\pi} = g_\rho [-i4N_c g^2 \int (p^2 - m_q^2)^{-2} \bar{d}^4 p] = g_\rho \quad (7·1)$$

via the LDGE (2·1). While the individual udu and dud quark graphs of Figs.8 are both linearly divergent, when added together with vertices  $g_{\rho^0 uu} = -g_{\rho^0 dd}$ , the net  $g_{\rho\pi\pi}$  loop in Fig.8 is log divergent. Equation(7·1) is Sakurai's VMD universality condition. Also a  $\pi^+\sigma\pi^+$  meson loop added to the quark loops of Fig.8 gives<sup>7)</sup>

$$g_{\rho\pi\pi} = g_\rho + g_{\rho\pi\pi}/6 \text{ or } g_{\rho\pi\pi}/g_\rho = 6/5. \quad (7·2)$$

If one first gauges the LσM lagrangian, the inverted squared gauge coupling is related to the  $q^2 = 0$  polarization amplitude as<sup>3)</sup>

$$(g_\rho^{-2}) = \pi(0, m_q^2) = -8iN_c/6 \cdot \int (p^2 - m_q^2)^{-2} \bar{d}^4 p = (3g^2)^{-1} \quad (7·3)$$

by virtue of the LDGE(2·1). But since we know  $g = 2\pi/\sqrt{3}$ , eq.(7·3) requires  $g_\rho = \sqrt{3}g = 2\pi$ , reasonably near the observed values  $g_{\rho\pi\pi} \approx 6.05$  and  $g_\rho \approx 5.03$ .

The chiral KSRF relation for the  $\rho$  mass<sup>18)</sup>  $m_\rho^2 = 2g_{\rho\pi\pi}g_\rho f_\pi^2$  coupled with this LσM implies  $m_\rho^2 = 2(2\pi)^2 f_\pi^2 5/6 \approx (754 \text{ MeV})^2$ , close to the observed  $\rho$  mass.

### §8. Scalar nonet and the IMF

Although the SU(3) L $\sigma$ M is more than a simple extension of the SU(2) L $\sigma$ M<sup>19)</sup> (due to scalar and pseudoscalar mixing angles), one obtains kinematical insight to the SU(3) L $\sigma$ M masses by working in the IMF because then the important dynamical tadpoles are substantially suppressed<sup>20)</sup> using IMF squared masses<sup>21)</sup>.

Specifically, SU(6) equal splitting laws (ESLs) suggest

$$m_\kappa^2(806) - m_\sigma^2(650) = K^2(496) - \pi^2(138). \quad (8.1)$$

Since the nonstrange  $\eta$  mass is 759 MeV (average of  $\eta(547)$ ,  $\eta'(958)$ ), ESLs say<sup>21)</sup>

$$\sigma_{NS}^2(650) - \pi^2(138) = \kappa^2(806) - K^2(496) = a_0^2(990) - \eta_{NS}^2(759), \quad (8.2)$$

$$\kappa^2(802) - \sigma_{NS}^2(650) = \sigma_S^2(930) - \kappa^2(802). \quad (8.3)$$

Another approach is the dynamical NJL pattern<sup>19)</sup> away from the CL:

$$\sigma^2(680) = 4\hat{m}^2, \quad \kappa^2(820) = 4m_s\hat{m}, \quad \sigma_S^2(950) = 4m_s^2, \quad (8.4)$$

for  $m_s/\hat{m} \approx 1.45$  and  $\hat{m} \approx 340$  MeV, the nonstrange constituent quark mass away from the CL. From eqs.(8.1-8.4), one may infer a scalar nonet pattern  $\sigma_{NS}(650 - 680)$ ,  $\kappa(800 - 820)$ ,  $f_0(980)$ ,  $a_0(990)$ , close to phase shift considerations<sup>16)</sup>.

It is interesting that the early  $qq\bar{q}\bar{q}$  bag model suggested a similar scalar nonet pattern<sup>22)</sup>  $\sigma(690)$ ,  $\kappa(880?)$ ,  $f_0(980)$ ,  $a_0(984)$ , Moreover a unitarized coupled channel meson analysis<sup>23)</sup> obtains a scalar nonet  $\sigma(500)$ ,  $\kappa(730)$ ,  $a_0(970)$ ,  $f_0(990)$ .

### §9. L $\sigma$ M as infrared limit of nonperturbative QCD

We suggest five links between the L $\sigma$ M and the infrared limit of QCD.

- i) Quark mass: the L $\sigma$ M has  $m_q = f_\pi \frac{2\pi}{\sqrt{3}} \approx 325$  MeV, while QCD has<sup>24)</sup>  $m_{dyn} = (\frac{4\pi\alpha_s}{3} < -\bar{\Psi}\Psi >_{1\text{GeV}})^{1/3} \approx 320$  MeV at a 1 GeV near-infrared cutoff.
- ii) Quark condensate: the L $\sigma$ M condensate is at infrared cutoff  $m_q$ <sup>25)</sup>:

$$< -\bar{\Psi}\Psi >_{m_q} = i4N_c m_q \int \frac{\bar{d}^4 p}{p^2 - m_q^2} = \frac{3m_q^2}{4\pi^2} \left[ \frac{\Lambda^2}{m_q^2} - \ln \left( \frac{\Lambda^2}{m_q^2} + 1 \right) \right] \approx (209\text{MeV})^3,$$

while the condensate in QCD is  $< -\bar{\Psi}\Psi >_{m_q} = 3m_{dyn}^3/\pi^3 \approx (215\text{MeV})^3$ .

- iii) Frozen coupling strength: the L $\sigma$ M coupling is for  $g = 2\pi/\sqrt{3}$  or  $\alpha_{L\sigma M} = \frac{g^2}{4\pi} = \frac{\pi}{3}$ , while in QCD  $\alpha_s = \frac{\pi}{4}$  at infrared freezeout<sup>26)</sup> leads to  $\alpha_s^{eff} = (4/3)\alpha_s = \pi/3$ .
- iv)  $\sigma$  mass: the L $\sigma$ M requires  $m_\sigma = 2m_q$ , while the QCD condensate gives<sup>27)</sup>  $m_{dyn} = \frac{g_{\sigma q\bar{q}}}{m_\sigma^2} < -\bar{\Psi}\Psi >_{m_\sigma}$  for  $\alpha_s(m_\sigma) \approx \pi/4$ , or  $m_\sigma^2/m_{dyn}^2 = \pi/\alpha_s(m_\sigma^2) \approx 4$ .
- v) Chiral restoration temperature  $T_c$ : the L $\sigma$ M requires<sup>28)</sup>  $T_c = 2f_\pi \approx 180$  MeV, while QCD computer lattice simulations find<sup>29)</sup>  $T_c = (150 \pm 30)$  MeV.

## §10. Conclusion

In §2, 3, the SU(2) L $\sigma$ M lagrangian was dynamically generated in all (chiral) regularization schemes, via loop gap equations, predicting the NJL  $\sigma$  mass  $m_\sigma = 2m_q$  along with meson-quark coupling  $g = 2\pi/\sqrt{N_c}$ . Then the three-and four-point quark loops were shown to “shrink” to tree graphs, giving the meson cubic and quartic couplings  $g' = m_\sigma^2/2f_\pi$ ,  $\lambda = 8\pi^2/N_c$ . Next in §4, the Nambu-Goldstone theorem (NGT) was shown to hold in L $\sigma$ M loop order with the pion charge radius  $r_\pi = 1/m_q$ . In §5, the SU(2) L $\sigma$ M requires color number  $N_c=3$  in loop order, then predicting  $m_q \approx 325$  MeV,  $m_\sigma \approx 650$  MeV,  $g \approx 3.63$ ,  $\lambda \approx 26$ ,  $r_\pi \approx 0.6$  fm in the CL.

In §6, we considered L $\sigma$ M chiral cancellations, both in tree and in loop order. Next, in §7, Sakurai’s vector meson dominance (VMD) empirically accurate scheme follows from the L $\sigma$ M, the latter further predicting  $g_{\rho\pi\pi} = 2\pi$  and  $g_{\rho\pi\pi}/g_\rho = 6/5$  along with the KSRF relation. Then in §8, a global extension of the SU(2) L $\sigma$ M to SU(3) was found in the infinite momentum frame (IMF). Finally in §9, we suggested that the L $\sigma$ M is the infrared limit of nonperturbative QCD.

## References

- [1] M. Gell-Mann and M. Levy, Nuovo Cimento **16** (1960), 705; V. de Alfaro, S. Fubini, G. Furlan and C. Rossetti, Currents in Hadron Physics (North Holland, 1973), chap. 5.
- [2] T. Hakioglu and M.D. Scadron, Phys. Rev. **D42** (1990), 941; **D43** (1991), 2439.
- [3] R. Delbourgo and M.D. Scadron, Mod. Phys. Lett. **A10** (1995), 251; R. Delbourgo, A. Rawlinson, and M.D. Scadron, *ibid.*, **A13** (1998) 1893.
- [4] A. Salam, Nuovo Cimento **25** (1962), 224; S. Weinberg, Phys. Rev. **130** (1963), 776; M.D. Scadron, Phys. Rev. **D57** (1998), 5307.
- [5] Y. Nambu and G. Jona-Lasinio, Phys.Rev. **122** (1961), 345 (NJL); also see Y. Nambu, Phys.Rev.Lett. **4** (1960), 380.
- [6] T. Eguchi, Phys.Rev. **D14** (1976), 2755; **D17** (1978), 611.
- [7] A. Bramon, Riazuddin and M.D. Scadron, J.Phys.G **24** (1998), 1.
- [8] R. Tarrach, ZPhys.C**2** (1979), 221; S.B.Gerasimov, Sov.J.Nucl.Phys. **29** (1979) 259.
- [9] A.F. Grashin and M.V. Lepeshkin, Phys.Lett.**B146** (1984), 11.
- [10] B.W. Lee, Chiral Dynamics, (Gordon and Breach, NY, 1972), p. 12.
- [11] S. Weinberg, Phys.Rev.Lett. **17** (1966), 616.
- [12] M.D. Scadron, Eur.Phys.J. **C6** (1999), 141.
- [13] R. Kamiński, *et. al.* Z Phys.C **74** (1997), 79.
- [14] A.N. Ivanov, M. Nagy, and M.D. Scadron, Phys.Lett.B **273** (1991), 137.
- [15] L.R. Babukhadia, *et. al.*, Phys.Rev.D **62** (2000) in press.
- [16] S. Ishida, *et. al.*, Prog. Theor.Phys. **95** (1996), 745; **98** (1997), 621.
- [17] See eg. P.Ko and S. Rudaz, Phys.Rev.D **50** (1994), 6877.
- [18] K. Kawarabayashi and M. Suzuki, Phys.Rev.Lett.**16** (1966), 255; Riazuddin and Fayyazudin, Phys.Rev.**147** (1966), 1071 (KSRF).
- [19] R. Delbourgo and M.D. Scadron, Int. J.Mod.Phys.A **13** (1998), 657.
- [20] S. Fubini, G. Furlan, Physics **1** (1965), 229; M.D. Scadron, Mod.Phys.Lett.**A7** (1992), 669.
- [21] See eg. M.D. Scadron, Phys. Rev. **D26** (1982), 239.
- [22] R.L. Jaffe, Phys. Rev. **D15** (1997), 267, 281; J.J. DeSwart, Hawaii conf. 1993.
- [23] E.van Beveren *et al.* Zeit. Phys. **C30** (1986), 615.
- [24] V. Elias and M.D. Scadron, Phys. Rev. **D30** (1984), 647.
- [25] L.R. Babukhadia, V. Elias and M.D. Scadron, J.Phys.G **23** (1997), 1065.
- [26] A. Mattingly and P. Stevenson, Phys.Rev.Lett. **69** (1992), 1320.
- [27] V. Elias and M.D. Scadron, Phys.Rev.Lett. **53** (1984), 1129.
- [28] N. Bilic, J. Cleymans and M.D. Scadron, Intern. J. Mod. Phys. **A 10** (1995), 1160.
- [29] Particle Data Group (PDG), C. Caso, *et.al.*, Eur.J.C **3** (1998), 1.